

with a two-electron reduction of the surface in either case. The heterolytic species may be photoexcited to the homolytic mode and undergo the same subsequent reactions. The barrier to methyl radical diffusion over O^{2-} sites is approximately the same as the desorption energy, ~ 0.4 eV. Homolytic adsorption at O^- sites on the basal planes will take place with the electron-hole pair excitation energy stored as Mo^V and the same catalyst reducing reactions forming ethane and formaldehyde will occur. Unless H_2CO is desorbed, additional electron-hole pair excitations should lead to further dehydrogenation and surface reduction with the formation of CO and CO_2 as seen in ref 1.

When O^- is present at the surface as a result of cation vacancies, homolytic and heterolytic products are comparable in stability at the edge sites, with the latter slightly favored. Homolytic adsorption will also take place at O^- sites on the basal planes. The methyl radical will be mobile over the O^{2-} basal plane sites but when it comes to an O^- it will bind as methoxy, being trapped by ~ 2.5 eV, the electron-hole pair recombination energy. In the

presence of an adjacent O^- , activated hydrogen loss from methoxy as in ref 8 is possible, resulting in the formation of formaldehyde, OH^- , and Mo^V . Additional O^- sites should activate the CH bonds in formaldehyde to yield more highly oxidized products.

These conclusions may be expected to apply to other systems such as the V^{5+} , P^{5+} , and Ti^{4+} supported oxide catalysts studied by Kazansky and co-workers.¹ The presence of O^- due to non-stoichiometry or UV charge-transfer excitation resulted in the reaction of methane to form various amounts of ethane, formaldehyde, carbon monoxide, and carbon dioxide. The variations in products for these catalysts and MoO_3 suggest their is much to learn about the effects of surface structure on the various reactions. Reference 1 states "It will be impossible to understand the photocatalytic reactions of paraffins, without a thorough study of their specific interactions with hole centers of the O^- type". We feel that the electronic aspects are now clear from the perspective of molecular orbital theory and that future characterization using surface science techniques will help clarify the structural effects.

Photochemical Methods for Characterizing the Nature of Polymer Aggregates in Aqueous Solutions and on a Silica Surface

Ping-Lin Kuo, Masami Okamoto,[†] and Nicholas J. Turro*

Chemistry Department, Columbia University, New York, New York 10027 (Received: November 4, 1986)

The nature and structure of the aggregates formed by a water-soluble poly(ethylene oxide-propylene oxide-ethylene oxide) block copolymer adsorbed on silica particles have been investigated by photoluminescence probe methods. The micropolarity and the aggregation number of the polymer aggregates adsorbed on silica particles were determined by fluorescence methods using pyrene as a probe and were found to be significantly smaller than those of the aggregates in aqueous solution. The aggregates adsorbed on silica have a higher solubilization ability and a higher ability of protecting pyrene from quenching by Cu^{2+} . The decay curves of pyrene in the aggregates on silica are similar to those observed in surfactant micelles. These results suggest that, relative to the solution phase, the polymer aggregates on the silica surface are smaller and more compact and possess properties similar to surfactant micelles. The entrance and exit rates for Cu^{2+} in the polymer aggregates on silica and in the solution phase are determined from the decay of pyrene fluorescence in the presence of Cu^{2+} . The values of these kinetic parameters are compared to those of pyrene in SDS micelles and are interpreted in terms of the size and water content of the polymer aggregates in two phases and in terms of the interaction between Cu^{2+} and the silica surface.

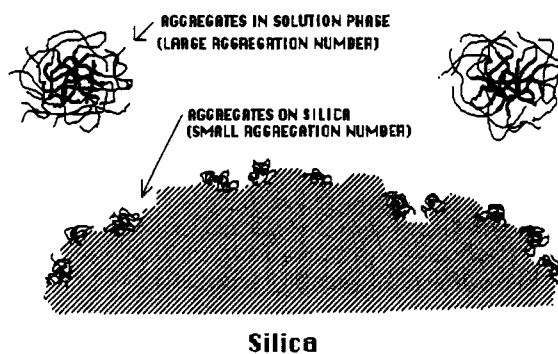
Introduction

The poly(ethylene oxide-propylene oxide-ethylene oxide) block copolymers (EPE) are composed of hydrophobic poly(propylene oxide) (PPO) and hydrophilic poly(ethylene oxide) (PEO) segments. Ordinary hydrophilic (water-soluble) polymers are extended by water and assume structures possessing random-coil chains. An increase in polymer concentration increases the mutual interaction of polymer chains. Due to the different solubilities in water of the PPO and PEO segments, the EPE block copolymer forms polymer aggregates with internal PPO segments surrounded by PEO segments.¹ Upon a further increase of the concentration of the polymer, the structure of these aggregates changes from monomolecular aggregates to polymolecular aggregates.² Thus, the structure and the properties of EPE polymer aggregates in aqueous solutions changes as a function of polymer concentration.

Both polyoxyethylenated nonionic surfactants and PEO are adsorbed on negatively charged silica as a result of hydrogen bonding between the $-SiOH$ groups of the silica surface and the oxygen atoms of the oxyethylene group.³ A similar interaction between EPE polymer and silica is expected, but the resulting structure and properties of EPE polymers adsorbed on silica may be quite different from those in the solution phase.

Various methods have been employed to measure the thickness of the adsorption layers,⁴ but the size of the aggregate formed by an adsorbed surfactant on a solid surface cannot be readily

SCHEME I: Sketch of the Aggregates of EPE Block Copolymer on the Silica Surface and in Solution Phase



determined by conventional methods such as light scattering. On the other hand, photochemical methods have been widely employed to study the structures and the properties of surfactant and/or polymer aggregates in aqueous solution containing surfactant and

(1) (a) Sandron, C. *Angew. Chem., Int. Ed. Engl.* **1963**, *2*, 248. (b) Tuzar, Z.; Kratochvil, P. *Adv. Colloid Interface Sci.* **1976**, *6*, 201. (c) Ikemi, M.; Odagiri, N.; Tanaka, S.; Shinohara, I.; Chiba, A. *Macromolecules* **1982**, *15*, 281.

(2) Prasad, K. N.; Luong, R. T.; Florence, A. T.; Paris, J.; Vaution, C.; Puisieux, F. *J. Colloid Interface Sci.* **1979**, *69*, 225.

(3) Rupprecht, H.; Liebl, H. *Kolloid. Z. Z. Polymn.* **1982**, *250*, 719.

(4) (a) Garvey, M. J.; Tadros, Th. F.; Vincent, B. J. *J. Colloid Interface Sci.* **1976**, *55*, 440. (b) Schentjens, J. N. H. M.; Fleer, G. J. *J. Phys. Chem.* **1979**, *83*, 1619.

[†] Present address: Technical College, Kyoto Institute of Technology, Matsugasaki, Sakyo-Ku, Kyoto 606, Japan.

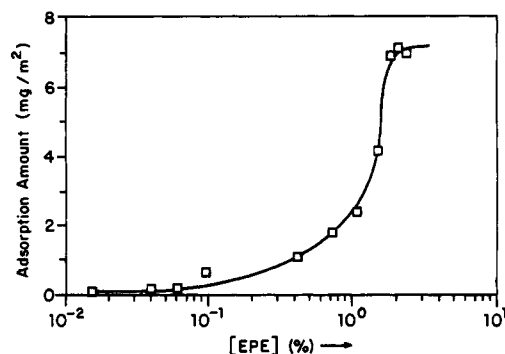


Figure 1. Adsorption isotherm of EPE on silica.

solid particles.⁵ The fluorescence probe method can provide information⁶ on the structure of the adsorbed surfactant. In this study, the structure and the properties of EPE aggregates adsorbed on a silica surface and dissolved in the solution phase (Scheme I) were investigated by photochemical methods. These results are compared with each other and discussed in terms of the interaction between the EPE polymer and the silica surface and the resulting structures which result from these interactions.

Experimental Section

Materials. Pyrene (Aldrich Chemical Co.) was recrystallized from ethanol three times. The synthesis of 1,3-dinaphthylpropane (DNP) has been reported in the literature.⁷ The silica (Analabs Co.) employed possessed a pore size of 1250 Å, a surface area of 25 m²/g, and a particle size of 40–100 μm. The poly(ethylene oxide-propylene oxide-ethylene oxide) block copolymer (EPE), possessing a ratio of ethylene oxide to propylene oxide of 0.8 (M_w 2917), was a product of Polysciences Co. Tannic acid, sodium chloride, and cupric sulfate (Aldrich Chemical Co.) were used as supplied.

Methods. A series of concentrations of EPE solutions (10 mL), containing an excess of pyrene, were stirred overnight, and then the undissolved material was filtered to prepare a pyrene-saturated EPE solution. To these solutions was added 0.2 g of silica, and a concentrated pyrene methanol solution was further added until the supernatant became slightly turbid. The resulting slurry was shaken overnight. The amount of pyrene adsorbed on the silica was calculated from the residual optical density (OD) of the supernatant. The concentration of EPE solution was determined from the turbidity titration of tannic acid⁸ according to a calibration curve. The amount of adsorption of EPE on silica was calculated from the change in the EPE concentration in the solution phase after the adsorption of EPE on silica.

All fluorescence measurements were recorded on a SLM instrument Model 8000 spectrometer. The ratio of the intensity of pyrene emission at 373 and 383 nm is defined as I_1/I_3 . The ratio of naphthyl excimer emission (I_e ca. 397 nm) to naphthyl monomer emission (I_m ca. 337 nm) is defined as I_e/I_m . The emissions were excited at 290 nm. The conversion of I_e/I_m into microviscosities follows a literature method.⁹ A single photon counting technique¹⁰ was used to determine fluorescence lifetimes.

Results

In the presence of surfactant micelles, the UV absorption of pyrene shifts slightly to longer wavelengths, e.g., the absorption maximum at 334 nm shifts to 337 nm. In solutions of EPE (0.02%

TABLE I: Solubilization Amount of Pyrene in the EPE Aggregates in Solution Phase and on Silica under Different EPE Concentrations

	EPE, %					
	2	1.7	1	0.1	0.07	0.02
solution phase ($\times 10^{-9}$ mol) ^a	114	79	46	14	11	8
silica ($\times 10^{-9}$ mol)	452	418	290	194	104	88

^a Pyrene was saturated in EPE solution.

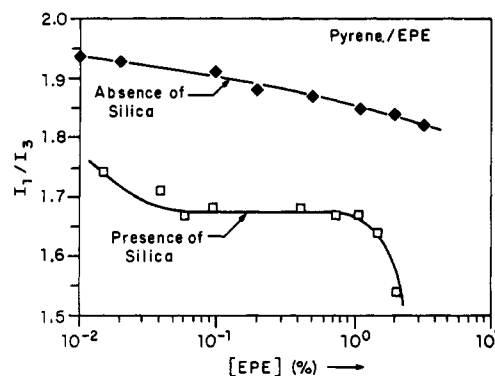


Figure 2. I_1/I_3 values of pyrene in the aggregates of EPE in the solution phase and on silica as a function of EPE concentration. Pyrene concentrations are the maximum solubilization amounts at different [EPE].

and 1%), the maximum absorptions of pyrene are 334 and 337 nm, respectively, which is consistent with the absence and the presence of EPE aggregates at 0.02% and 1%, respectively. In a 0.4% EPE aqueous solution, the adsorption of pyrene occurs at 337 nm, indicating the presence of polymer aggregates. When silica is added to the solution, however, the UV absorption of pyrene in the supernatant shifts from 337 to 334 nm. The shift in wavelength is interpreted to result from the disappearance of aggregates in supernatant due to the adsorption of EPE on silica. Figure 1 shows an adsorption isotherm of EPE on silica based on the amount of pyrene remaining in the supernatant. A small, constant adsorption is observed below 0.1% EPE which then increases rapidly and then tends to level off. The extent of adsorption is higher than typically observed for water-soluble polymers.^{11,12} This higher adsorption is interpreted to mean that EPE aggregates at the silica-solution interface have a higher solubilizing efficiency than the aggregates in the solution phase.

Table I shows the extent of maximum solubilization of pyrene in the EPE aggregates in the solution phase and in the EPE aggregates adsorbed on the silica surface. In the solution phase, the limiting pyrene saturated concentration increases as the EPE concentration increases from 0.02% to 2%. The maximum concentration of pyrene in 0.02% EPE (5.6×10^{-6} M) is similar to that in water, and the concentration of pyrene in 2% EPE is much smaller than that for a nonionic surfactant $C_{12}PhE_{10}$ solution (i.e., ca. 1×10^{-4} M), indicating the low solubilization ability of EPE aggregates in the solution phase. On the silica surface, however, the extent of pyrene solubilization of EPE aggregates significantly increases by a factor of 4–10.

The parameter I_1/I_3 of pyrene emission has been used to monitor the micropolarity experienced by pyrene⁵ in colloidal aggregates. The I_1/I_3 value increases with increasing micropolarity. Figure 2 shows the I_1/I_3 value of pyrene as a function of EPE concentration in the absence of presence of silica. As the EPE concentration increases, in the solution phase, I_1/I_3 values remain relatively constant at ca. 1.9 (waterlike environment) below 0.2% and then decrease slightly to ca. 1.8 at 2% EPE. In the presence of silica, I_1/I_3 decreases from 1.74 to 1.68 in the range

(5) (a) Thomas, J. K. *Chem. Rev.* **1980**, *80*, 283. (b) Singer, L. A. In *Solution Behavior in Surfactants*; Mittal, K. L., Fendler, E. J., Eds.; Plenum: New York, 1982; Vol. 1, p 73. (c) Turro, N. J.; Baretz, B. H.; Kuo, P. L. *Macromolecules* **1984**, *17*, 1321. (d) Turro, N. J.; Kuo, P. L.; Somasundaran, P.; Wong, K. J. *J. Phys. Chem.* **1986**, *90*, 288.

(6) (a) Levitz, P.; Damme, H. V.; Keravis, D. *J. Phys. Chem.* **1984**, *88*, 228. (b) Levitz, P.; Damme, H. V. *J. Phys. Chem.* **1986**, *90*, 1302.

(7) Chandross, E. A.; Dempster, C. J. *J. Am. Chem. Soc.* **1970**, *92*, 3586.

(8) Attia, Y. A.; Rubio, J. *Br. Polym. J.* **1975**, *7*, 135.

(9) Avouris, P.; Kordas, J.; El-Bayoumi, M. A. *Chem. Phys. Lett.* **1974**, *26*, 373.

(10) Turro, N. J.; Aikawa, M. *J. Am. Chem. Soc.* **1980**, *102*, 4866.

(11) (a) Dick, S. G.; Fuerstenau, D. W.; Healy, T. W. *J. Colloid Interface Sci.* **1971**, *37*, 595. (b) Wakamatsu, T.; Fuerstenau, D. W. In *Absorption from Aqueous Solution*; Weber, W. J., Matijevic, E., Eds.; American Chemical Society: Washington, DC, 1968; p 161.

(12) Killmann, E.; Gutling, N.; Wild, Th. In *Polymer Adsorption and Dispersion Stability*; Goddard, E. D., Vincent, B., Eds.; American Chemical Society: Washington, DC, 1984; p 537.

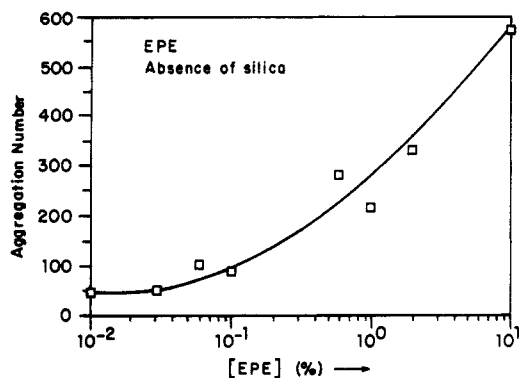


Figure 3. Aggregation number of the EPE aggregates in solution as a function of EPE concentration.

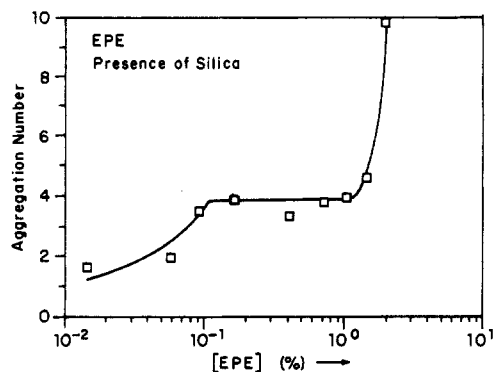


Figure 4. Aggregation number of EPE aggregates adsorbed on silica as a function of EPE concentration.

0.02–0.06% EPE and remains constant at 1.68 in the range of EPE ca. 0.06–1%. Upon further increase of EPE concentration the value of I_1/I_3 decreases to 1.54 (alcohol-like environment).

The monomer fluorescence decay of pyrene in EPE aggregates was fit¹³ to

$$\ln(I(t)/I(0)) = n(e^{-k_1 t} - 1) - k_1 t \quad (1)$$

where n is the occupancy number of pyrene in EPE polymer aggregates and k_1 and k_e are the rate constant of fluorescence decay and excimer formation in micellar solution, respectively. The aggregation number of EPE in the solution phase can be evaluated from

$$\text{agg no.} = n[\text{EPE}]/[\text{P}]M_w \quad (2)$$

Similarly, the aggregation number of EPE on silica can be calculated from a knowledge of the adsorbed amount of EPE and pyrene on silica (EPE_{ads} and P_{ads}) and the M_w of EPE.

$$\text{agg no.} = n\text{EPE}_{\text{ads}}/\text{P}_{\text{ads}}M_w \quad (3)$$

From the above analysis, the aggregation number of EPE in the solution phase (35–600) is found to be much larger than that in the adsorption layer (2–9). In the solution phase, the aggregation number monotonically increases with EPE concentration (Figure 3). On the silica surface, the aggregation number increases with increasing EPE concentration but remains constant over a wide range (ca. 0.1–1%, Figure 4).

The fluorescence decay of pyrene was used to study the kinetic properties of a cation (Cu^{2+}) dissolved inside the EPE aggregates on the silica surface or in the solution phase. Figure 5 shows the pyrene fluorescence decay for several systems. In water, Cu^{2+} quenches the pyrene fluorescence, and the decay is exponential. In SDS micelles, the decay curve can be analyzed as being composed of a transient multiexponential decay and a single-exponential decay. The multiexponential decay is ascribed to the

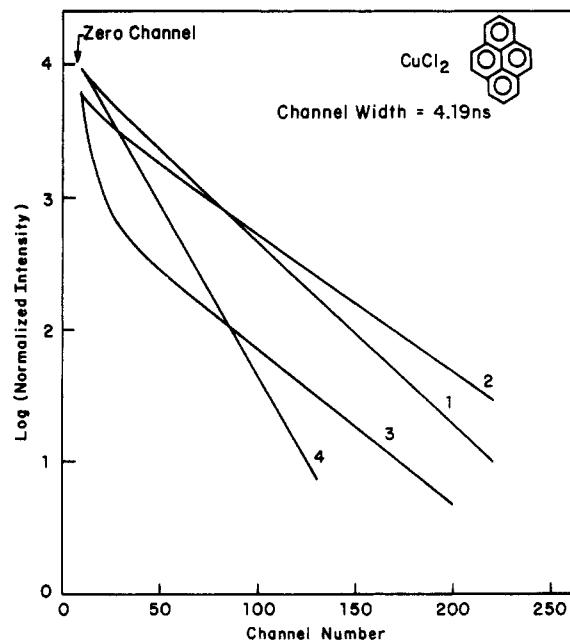


Figure 5. Decay curves of pyrene quenched by Cu^{2+} in (1) the aggregates of EPE in the solution phase, (2) the aggregates of EPE on silica, (3) SDS micelles, and (4) water.

well-established decay pattern of pyrene in micelles.¹⁴ In the EPE aggregates in the solution phase, the decay is not strictly exponential but is similar to that in water. The decay is, however, clearly much slower in the EPE system. The nonexponential nature of the decay of pyrene in EPE aggregates on silica is more apparent than that in the solution phase but less obvious than that in SDS micelles.

In micelles, the decay curve of pyrene fluorescence in the presence of quencher follows eq 4 according to the quenching model¹⁴

$$\ln(I(t)/I(0)) = -A_2 t + A_3[e^{-A_4 t} - 1] \quad (4)$$

$$A_2 = k_f + S_2[Q] \quad (5)$$

$$A_3 = S_3[Q] \quad (6)$$

$$1/S_2 = 1/k_+ + (1/k_-)[M] \quad (7)$$

$$1/S_3 = k_-/k_+ + [M] \quad (8)$$

where k_f is the rate constant of fluorescence, $[Q]$ is the quencher concentration, $[M]$ is the micellar concentration, and k_+ and k_- are the entrance and exit rate constants of quencher into and out of the micelles. The decay curves of pyrene in the solution phase and on the silica surface under a series of concentrations of Cu^{2+} were fitted to eq 4 by computer to acquire A_2 and A_3 values. The $1/A_2$ value relates to the lifetime of pyrene in the presence of quencher, and the A_3 value relates to the effectiveness of quenching. The lifetime of pyrene ($1/A_2$) in different systems (Figure 5) in the presence of 1.6×10^{-3} M Cu^{2+} is evaluated as 132 ns in EPE aggregates in the solution phase, 193 ns in the EPE aggregates on silica, 154 ns in SDS micelles, and 71 ns in water, respectively. The EPE aggregates on silica more effectively protect pyrene from quenching than the EPE aggregates in the solution phase.

For 2% EPE solution, the A_2 values and A_3 values for EPE aggregates in the solution phase and on the silica surface are shown as a function of quencher concentration in Figure 6. The slope for A_2 in the solution phase is bigger than that on silica surface. For 0.2% EPE solution, the A_3 value increases with increasing Cu^{2+} concentration for EPE on silica surface but remains constant for EPE in solution phase. As the EPE concentration decreases, the decay curve of pyrene in EPE aggregates in the solution phase

(13) (a) Atik, S. S.; Nam, M.; Singler, L. A. *Chem. Phys. Lett.* **1979**, *67*, 75. (b) Linos, P.; Lang, J.; Strazielle, C.; Zana, R. *J. Phys. Chem.* **1982**, *86*, 1019.

(14) Dederen, J. C.; Van der Auweraer, M.; DeSchryver, F. C. *Chem. Phys. Lett.* **1979**, *68*, 451.

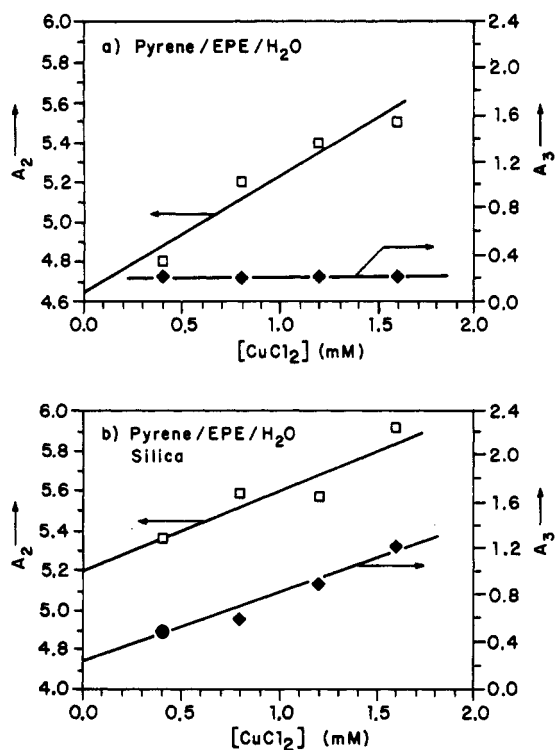


Figure 6. A_2 and A_3 values for the pyrene decay quenched by Cu^{2+} as a function of CuCl_2 concentration in the EPE aggregates (a) in the solution phase and (b) on silica.

is close to a straight line with the A_3 value close to zero, which is the A_3 value in water (e.g., 0.15 for 1.5%, 0.087 for 0.7%, and 0.0084 for 0.4%). For the adsorption layer, the trends of A_2 and A_3 observed for 2% become less regular probably due to the small size of the aggregate.

According¹⁴ to eq 5–8, k_+ and k_- for the EPE adsorbed on silica surface can be calculated from the knowledge of $[M]$. The results obtained are $k_+ = 1.4 \times 10^8 \text{ M}^{-1} \text{ s}^{-1}$ and $k_- = 2.2 \times 10^5 \text{ s}^{-1}$.

Since A_3 is independent of quencher concentration, k_+ and k_- for EPE in the solution phase cannot be calculated as mentioned above. For EPE in the solution phase, S_2 with a given $[M]$ can be similarly acquired from eq 7. According to eq 7, by changing $[M]$, $1/k_+$ and $1/k_-$ can be acquired from the intercept and the slope of the plot of $1/S$ vs. $[M]$, respectively. The results obtained are $k_+ = 1.3 \times 10^8 \text{ M}^{-1} \text{ s}^{-1}$ and $k_- = 1.6 \times 10^4 \text{ s}^{-1}$.

Discussion

In our experiments, pyrene may reside in EPE aggregates adsorbed on the silica surface or in EPE aggregates in the solution phase. The amount of pyrene in the aqueous phase is negligible. To a sample for measurement which contains 0.2 g of silica and 0.36 g of supernatant, the amount of pyrene in the adsorption layer and in the solution phase can be estimated. For example, for the sample prepared from the solution of 2% EPE, the OD of pyrene in the solution phase decreased from 1.12 to 0.12 after the addition of silica. This allows the calculation of the amount of pyrene in the adsorption layer and in the solution phase to be 2.3×10^{-7} and 9.7×10^{-10} mol, respectively. It is clear that the amount of pyrene solubilized in the solution phase is much lower than that on silica surface. Therefore, the fluorescence measurement for the sample containing both the adsorption layer and the solution phase can be assumed to result from the adsorption layer.

The parameter I_1/I_3 has been used to monitor the micropolarity experienced by pyrene. The micropolarity can be related to the structure of EPE aggregates; i.e., the more contracted the polymer chain, the lower micropolarity (the lower I_1/I_3 value) the pyrene reports.¹⁵ For the EPE aggregates in solution phase, I_1/I_3 decreases monotonically with increasing EPE concentration, sug-

gesting that EPE aggregates become more compact as the polymer concentration increases due to the mutual perturbation of polymer chains. This is the usual behavior of such polymers in an aqueous solvent. For EPE aggregates on a silica surface, the change in micropolarity upon increasing EPE concentration is significantly larger than that observed in solution phase. We propose that this is due to the interaction between polymer and silica which causes the polymer to be more contracted on the silica surface. The microviscosity of EPE aggregates in the solution phase and on silica surface determined by DNP method are 37 and 65 cP, respectively. This result is also consistent with a compact structure of EPE aggregates on silica surface.

In the solution phase, the size of EPE aggregates is relatively large with aggregation numbers in the range of 90–570 for EPE concentration of 0.02–2% (Figure 3). Since the EPE aggregates in aqueous solution are less closely packed than those of nonionic micelles, the micellar size of EPE in solution phase is much bigger than that of a conventional nonionic surfactant such as poly-(ethylene glycol) *n*-nonylphenyl ethers ($\text{C}_9\text{PhE}_{10}$) by a factor of more than 3–30. Our results indicate that the aggregation number of EPE adsorbed on a silica surface is significantly smaller than that in the solution phase. For example, in the EPE concentration range 0.1–1%, the aggregation number remains constant at ca 4. If the aggregate becomes too large, the polymers at the outer phase of the adsorption layer are beyond the influence of the local polymer–silica interaction responsible for adsorption and are forced into the solution phase and into equilibrium with the EPE on silica surface.

From the information provided by micropolarity, aggregation number, and the solubility characteristics deduced from our investigations, the following conclusions are reached: In solution phase, the EPE aggregates consist of polymer chains that are expanded by water and are very large. Relative to the solution phase, the EPE aggregates adsorbed on silica are much smaller and are significantly contracted as shown schematically in Scheme I.

Since the contracted polymer aggregates behave like surfactant micelles and have high solubilization ability, the difference in the structure between EPE on the silica surface and in solution phase also can be characterized by a different solubilization ability from that in solution phase (Table I), demonstrating that the polymer chain of EPE on silica is much more contracted and therefore more hydrophobic and better able to solubilize pyrene.

For EPE adsorbed on silica surface, the I_1/I_3 values remain constant in the concentration range 0.06–1% (Figure 2). This corresponds to the constant region in the plot of aggregation number vs. $[\text{EPE}]$ (0.1–1%, Figure 4). Thus, the structure of EPE on silica surface remains stable in this concentration range. The increase in EPE concentration in this range does not change the structure but only increases the concentration of aggregates on surface. Above this range, the increase in EPE concentration increases the aggregation number and decreases the I_1/I_3 value again. The continual decreasing I_1/I_3 suggests that the EPE aggregates keep on getting more compact as a result of the increase in aggregation number of EPE.

From pyrene decay experiments several results are obtained as follows. Relative to the EPE aggregates in the solution phase, for the EPE aggregates on silica (1) the shape of quenching decay curve is similar to that of surfactant micelles (Figure 5), (2) the quencher less efficiently decreases the lifetime of pyrene, and (3) A_3 values are significantly larger.

These results suggest that the structure of EPE aggregates on the silica surface is closer to SDS micelles as a result of the contracted polymer chains. This conclusion is identical with that determined by the measurement of micropolarity, aggregation number, and solubilization.

Relative to an SDS micelle (micellar weight ca. 17 300), the EPE aggregate in solution phase (the calculated micellar weight ca. 570 000) is significantly bigger, and its structure is significantly less compacted because of the water inside it. Therefore, it is reasonable to expect that Cu^{2+} resides longer inside EPE aggregates than in SDS aggregates. This factor contributes to a smaller

k_- ($1.6 \times 10^4 \text{ s}^{-1}$) for Cu^{2+} in EPE aggregate than in SDS micelles ($1.2 \times 10^5 \text{ s}^{-1}$).¹⁶ Relative to EPE aggregates in solution phase, the micellar weight of EPE aggregates on silica (ca. 29 000) is close to that of SDS and it is more compact and contains less water; therefore, the k_- value for Cu^{2+} ($2.2 \times 10^5 \text{ s}^{-1}$) is similar to that in SDS.

For EPE aggregates on silica, the k_+ ($1.3 \times 10^8 \text{ M}^{-1} \text{ s}^{-1}$) value is similar to that ($1.4 \times 10^8 \text{ M}^{-1} \text{ s}^{-1}$) in solution phase; both are smaller than that in SDS ($1.2 \times 10^9 \text{ M}^{-1} \text{ s}^{-1}$).¹⁶ The smaller k_+ for EPE on silica surface is possibly related to the smaller diffusion of Cu^{2+} due to the interaction between Cu^{2+} and silica.

Conclusion

EPE block copolymers are adsorbed on silica, and the adsorption isotherm is similar to that for surfactants. The solubilization amount of pyrene in the polymer aggregates on silica is 4–10 times higher than that in the solution phase. The micropolarity inside the aggregate on silica surface ($I_1/I_3 = 1.54$ for 0.2% EPE) is significantly smaller than that in the solution phase ($I_1/I_3 = 1.84$). The aggregation numbers of the polymer aggregates on silica surface (2–9 for [EPE] = 0.01–2%) are significantly smaller than those in the solution phase (35–600). The lifetime of pyrene

quenched by Cu^{2+} in the aggregates on silica (193 ns) is higher than that in the solution phase (132 ns). The shapes of the decay curves of pyrene quenched by Cu^{2+} show that the nature of polymer aggregates on silica is closer to that of SDS micelles than to the polymer aggregates in solution phase. These results show that the polymer aggregates on silica surface are smaller and more contracted and possess properties close to those of SDS micelles. On silica, the flat regions in the plot of aggregation number vs. [EPE] and of I_1/I_3 vs. [EPE] are the same, indicating that the polymer aggregates on silica is stable with an aggregation number of ca. 4. The values of k_+ and k_- for Cu^{2+} in the EPE aggregates on silica are $1.4 \times 10^8 \text{ M}^{-1} \text{ s}^{-1}$ and $2.2 \times 10^5 \text{ s}^{-1}$, respectively, and those in the solution phase are $1.3 \times 10^8 \text{ M}^{-1} \text{ s}^{-1}$ and $1.6 \times 10^4 \text{ s}^{-1}$, respectively. Relative to the k_- of SDS ($1.2 \times 10^5 \text{ s}^{-1}$), the smaller k_- for polymer aggregates in the solution phase is attributed to the big size and the high water-enriched interior.

Acknowledgment. The authors thank the Army Research Office and the National Science Foundation for their generous support of this research. The important advice and assistance of Professor P. Somasundaran and Dr. Prem Chandar of Columbia University's School of Engineering and Applied Sciences (Henry Krumb School of Mines) are gratefully acknowledged.

Registry No. (EO)(PO)(block copolymer), 106392-12-5; SiO_2 , 7631-86-9; Cu^{2+} , 15158-11-9; pyrene, 129-00-0.

(16) Hashimoto, S.; Thomas, J. K. *Chem. Phys. Lett.* **1984**, *109*, 115.

Microstructure of Formamide Microemulsions from NMR Self-Diffusion Measurements

K. P. Das,*† A. Ceglie,‡ and B. Lindman*

Department of Physical Chemistry 1, Chemical Center, University of Lund, S-221 00, Lund, Sweden
(Received: December 3, 1986)

The microemulsion stability range and multicomponent self-diffusion data are presented for systems of formamide, alcohol, and sodium dodecyl sulfate in both the presence and absence of an oil, *p*-xylene; the alcohols used were 1-butanol, 1-pentanol, 1-hexanol, 1-heptanol, and 1-octanol. The results have been compared with the analogous water/alcohol/SDS systems. In the nonaqueous systems, high self-diffusion coefficients were observed for all the components in essentially all the regions studied. The results do not support any appreciable confinement of any component into closed domains. Rather the structure seems to be close to the structureless limit of simple solutions. The aqueous systems are structurally quite different from these nonaqueous solutions and show considerable surfactant organization in bicontinuous or droplet structures. Thus, distinct water droplets were found in the aqueous systems with primary alcohols having six or more carbons. The structure of the formamide system is, on the other hand, quite insensitive to the chain length of the alcohol. These conclusions about the nonaqueous and aqueous microemulsions remain valid in both the presence and absence of the oil, *p*-xylene. Structureless microemulsions have also been found by using as nonaqueous solvents *N*-methylformamide and *N,N'*-dimethylformamide in place of formamide. Self-diffusion measurements have also been extended to the two-component nonaqueous solvent/SDS systems. The results are again very different from those of the aqueous system and point to a quite insignificant aggregation with no evidence for distinct hard-core micelles. The results on organization in these nonaqueous systems are consistent with the recent findings of Rico and Lattes who have demonstrated that the organization in nonaqueous surfactant systems requires other choices of surfactant chain length, cosurfactant, and temperature than in aqueous systems.

Introduction

It has been known for a long time that surfactants can form aggregates also in nonaqueous solvents.¹⁻⁷ Micelle formation of different surfactants has been reported in a number of solvents like various amides,² dimethyl sulfoxides,² glycols,^{3,4} and even inorganic salt melts.^{5,6} Since hydrophobic interactions are responsible for micelle formation in an aqueous medium, analogous solvophobic interactions were postulated for nonaqueous media. However, a recent study by Almgren et al.⁸ using a large number of experimental techniques has raised doubts as to the existence of real aggregates of surfactant molecules in such media and

reported that unless there is the presence of sufficient water there is a poor organization of sodium dodecyl sulfate (SDS) in a nonaqueous solvent like formamide.

Among other organized surfactant assemblies, liquid crystals have been identified in nonaqueous solvents, for quite some time.

(1) *Solution Behaviour of Surfactants*, Vol. 2, Part III, Mittal, K. L., Fendler, E. J., Eds.; Plenum: New York, 1982; pp 743-886.

(2) Singh, H. N.; Saleem, S. M.; Singh, R. P.; Birdi, K. S. *J. Phys. Chem.* **1980**, *84*, 2191.

(3) Ray, R. *J. Am. Chem. Soc.* **1969**, *91*, 6511.

(4) Ionescu, L. G.; Fung, D. S. *J. Chem. Soc., Faraday Trans. 1* **1981**, *77*, 2907.

(5) Evans, D. F.; Kaler, E. W.; Benton, W. J. *J. Phys. Chem.* **1983**, *87*, 533.

(6) Evans, D. F.; Chen, S. H. *J. Am. Chem. Soc.* **1981**, *103*, 481.

(7) Evans, D. F.; Yamauchi, A.; Rohan, R.; Casassa, E. J. *J. Colloid Interface Sci.* **1982**, *88*, 89.

(8) Almgren, M.; Swarup, S.; Löfroth, J. E. *J. Phys. Chem.* **1985**, *89*, 4621.

* On leave from the Department of Chemistry, Vidyasagar College, 39, Shankar Ghosh Lane, Calcutta 700 006, India.

† Present address: Dipartimento di Chimica, Università degli Studi di Bari, Via Amendola 173, 70126 Bari, Italia.